Prediction of Wave and Wind induced Dynamic Response in Time Domain using RM Bridge

Johann Stampler, Jörg Sello, Mitja Papinutti

Bentley Systems Austria, Graz, Austria

Arne Bruer, Mathias Marley

TDA AS, Oslo, Norway

Johannes Veie, Simen Helgren Holtberget

Norwegian Public Roads Administration, Oslo, Norway

Contact: Johann.Stampler@Bentley.com

Abstract

This project is a feasibility study on a new bridge concept which is being investigated for crossing the 5 km wide Bjørnafjord on the west coast of Norway. The bridge concept consists of a 3-span suspension bridge, supported by two tension leg moored floaters midfjord and two bottom-fixed traditional concrete pylons near shore. The 3 main spans of the bridge have a length of 1385 m. The water depth is 550 m at one floater and 450 m at the other. Time domain analyses with coupled wind and wave loading have been performed in order to assess the bridge response due to environmental loading. The suspension bridge is designed and analysed using structural bridge software RM Bridge. New functionality for including hydrodynamic properties has been implemented in RM Bridge as part of the project.

Keywords: 3-span floating suspension bridge, hydrodynamics, radiation, aerodynamics, time domain analysis, wave loading

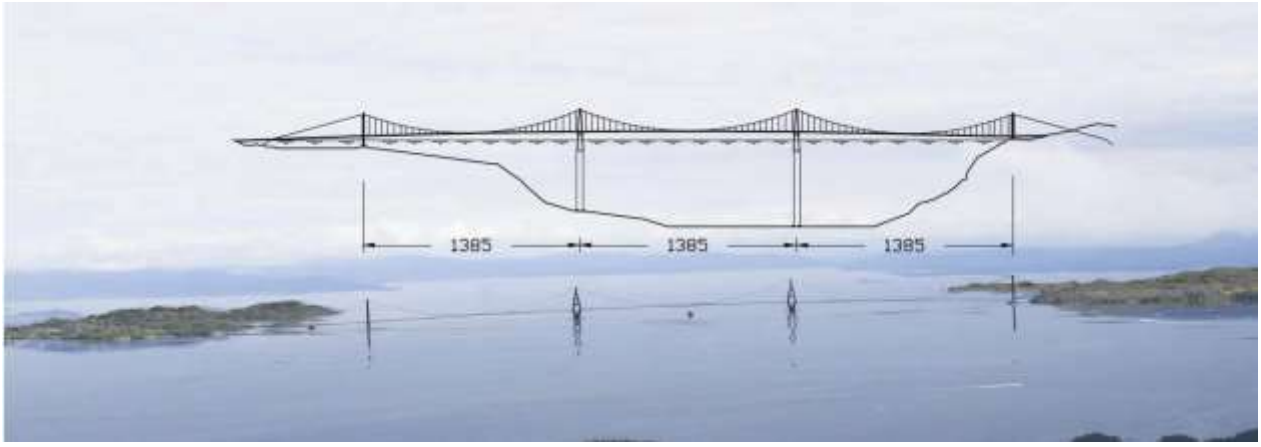

Figure 1. Overview of the bridge. Courtesy Norwegian Public Road Administration (NPRA)

1 Project Background

This project is a feasibility study on a new bridge concept [1], depicted in Figure 1 and Figure 2. The bridge concept consists of a 3-span suspension bridge, supported by two tension leg moored floaters and two fixed traditional concrete pylons.

The 3 main spans of the bridge have a length of 1385 m. The north approach bridge has a length of approximately 600 m from the concrete pylon to

Figure 2. 3D view of bridge depicting concept for floating foundations midfjord. Courtesy NPRA

the S-point in the spread saddle. The water depth is 550 m at one floater and 450 m at the other.

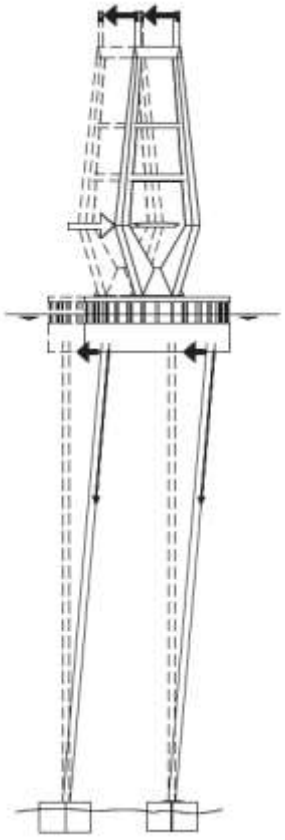

Figure 3. Sketch of TLP bridge concept showing horizontal restoring forces of tendons and cable system. Courtesy Arne J. Myhre (NPRA)

The tension leg platform (TLP) concept is used by the offshore industry to provide a stable working platform at large water depths. The tension legs (tendons) provide large stiffness in the vertical direction as well as for rotation about the two horizontal axes. The horizontal stiffness of the floater, depicted in Figure 3, is given by the total tension in the tendons as

$$k_{x,z} = \frac{buoyancy - weight}{tendon\ length} \quad (1)$$

where *buoyancy* is the net hydrostatic pressure acting on the floater and *weight* is the total weight supported by the floater. This means that the desired stiffness can be obtained by tuning the buoyancy and weight of the structure.

In addition there is significant stiffness offered by the superstructure in both horizontal directions. The geometric stiffness of the superstructure for mode 1 (half sine wave, see Figure 4) can, according to [1], be calculated approximately from the total pre-tensioning in the main cables as

$$k_z = \frac{horizontal\ cable\ force}{span\ length} \quad (2)$$

Figure 4. Geometric stiffness of the superstructure for mode 1. Courtesy Arne J. Myhre (NPRA)

Stiffness of the two floaters as well as geometric stiffness of the superstructure is shown in Table 1.

Table 1. Transversal bridge stiffness

Unit	Floater 1 (550m water depth)	Floater 2 (450m water depth)	Super-structure mode 1
Stiffness [MN/m]	0,40	0,51	0,21

The system has large inertia and is relatively flexible in the lateral direction, which means that wave loads are counteracted by inertial forces.

2 Analysis Model

The global analysis model, depicted in Figure 5, has been established in software RM Bridge. The pylon and superstructure including bridge deck, cable

system and hangers are modelled as structural elements. The submerged parts of the floaters are modelled as rigid bodies connected to the seabed by massless springs representing the tendons. The rigid body assumption is necessary for including hydrodynamic properties as point loads, and is sufficient for global response analysis as well as analysis of the superstructure and tendons.

Figure 5. Graphical representation of RM Bridge structural model showing TLP-supported Pylon

2.1 Hydrostatic properties

Buoyancy is modelled as a structurally fixed vertical force applied in the center of buoyancy. This ensures that the destabilizing moment of the buoyancy force for rotations about the x- and z-axis is included in the analysis. Hydrostatic restoring forces due to change in displaced volume are modelled as linear springs,

$$k_y = \rho g A_{wp} \quad (3)$$

$$k_{rx} = \rho g I_{zz,wp} \quad (4)$$

$$k_{rz} = \rho g I_{xx,wp} \quad (5)$$

where k_y is the stiffness coefficient for vertical displacement, k_{rx} and k_{ry} are the stiffness coefficients for rotation about x-axis and z-axis respectively. ρ is the density of water, g is the acceleration of gravity, A_{wp} is the water plane area, $I_{zz,wp}$ and $I_{xx,wp}$ are the second area moments of the water plane area about the x-axis and z-axis respectively.

2.2 Hydrodynamic radiation forces

Hydrodynamic properties of the hull are obtained from radiation/diffraction analysis using the Ansys AQWA software package [4].

Figure 6. Hydrodynamic panel model developed in Ansys AQWA for obtaining hydrodynamic and hydrostatic properties

The equation of motion of a body in water can be written as

$$[M + M_A(\omega)]\ddot{x} + C_A(\omega)\dot{x} + Kx = F_{wave} \quad (6)$$

where non-linear terms have been omitted for simplicity. x, $\dot{x}$, $\ddot{x}$ denote displacement, velocity and acceleration respectively. M is the structural mass and K is the stiffness provided by i.e. the waterplane area and mooring. $M_A(\omega) = M_A(\infty) + M_a(\omega)$ and $C_A(\omega)$ are the frequency-dependent hydrodynamic added mass and damping, as shown in Figure 7 for the transversal direction. F_{wave} is the excitation force from incoming waves, which is considered uncoupled from the motion of the body.

Equation 6 can be readily solved in the frequency-domain. However, to include nonlinear terms the equation of motion must be solved in the time domain. This can, according to [2], be done by representing the hydrodynamic radiation force with a convolution integral,

$$C(t) = \int_0^t R(t-\tau)\dot{x}(\tau)d\tau, \quad (7)$$

where

$$R(t) = \frac{2}{\pi}\int_0^\infty C_A(\omega)\cos(\omega t)d\omega \quad (8)$$

is the retardation function of the hydrodynamic radiation force.

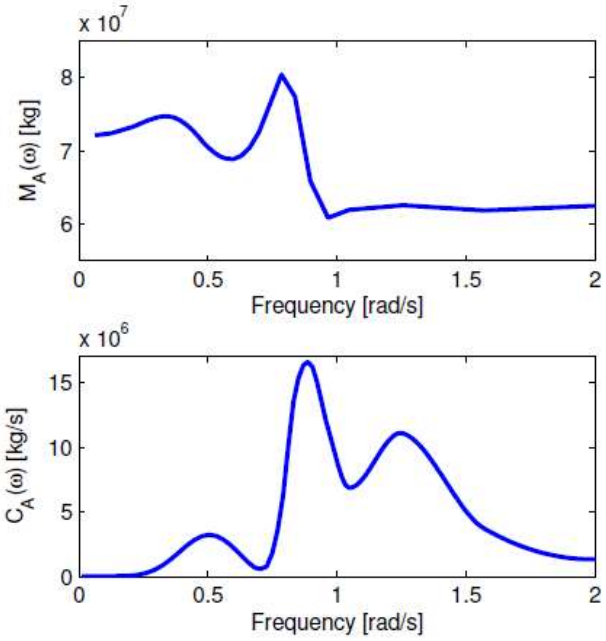

Figure 7. Added mass (top) and added damping (bottom) in the z-direction of the hull

The equation of motion now becomes

$$[M + M_A(\infty)]\ddot{x} + Kx = F_{wave} + C(t) \qquad (9)$$

where hydrodynamic radiation forces are included as an external force $C(t)$ on the right-hand side of the equation.

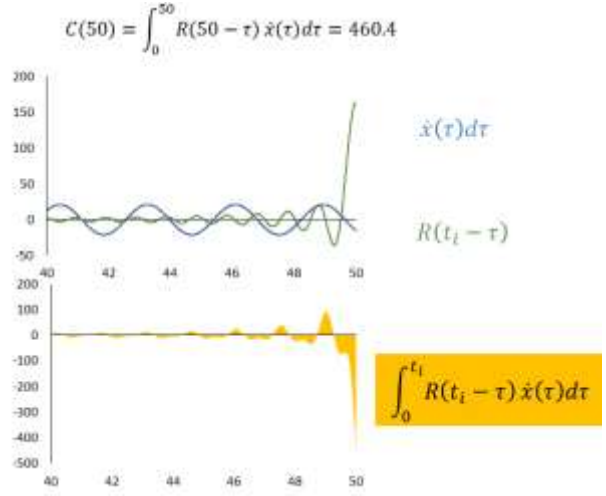

Figure 8. Retardation function (top) and convolution integral (bottom)

Since $C(t)$ is calculated from the velocity history it includes force contribution from both inertia $M_a(\omega)$ and damping $C_A(\omega)$. The process of obtaining $C(t)$ is shown graphically in Figure 8.

2.3 Hydrodynamic viscous forces

Hydrodynamic viscous drag and damping is modelled as

$$dF_{viscous} = \frac{1}{2}\rho C_d D(U_{element} - U_{current})^2 \qquad (10)$$

where $dF_{viscous}$ is integrated along the structural element to obtain the viscous force. C_d is the drag coefficient, D is the diameter, $U_{element}$ is the element velocity and $U_{current}$ is the current velocity. Hydrodynamic viscous drag is applied both to the hull and the tendons.

2.4 Hydrodynamic diffraction forces

First order wave loads are calculated externally prior to simulation from transfer functions providing the relation between surface elevation ζ and structural load F_{wave} (shown in Figure 9 for the z-direction). The incoming waves are modelled as a stochastic process from wave spectra representative of the Bjørnafjorden basin. Second order wave loads can be obtained in a similar manner, but that has not been done in the current study.

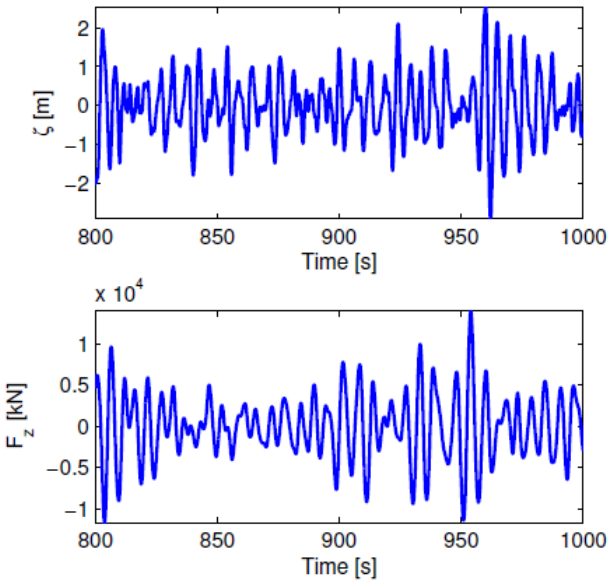

Figure 9. Surface elevation ζ and corresponding transversal wave load F_z

2.5 Aerodynamic drag

Aerodynamic loading is modelled in a simplified manner taking only wind-induced drag loads into account.

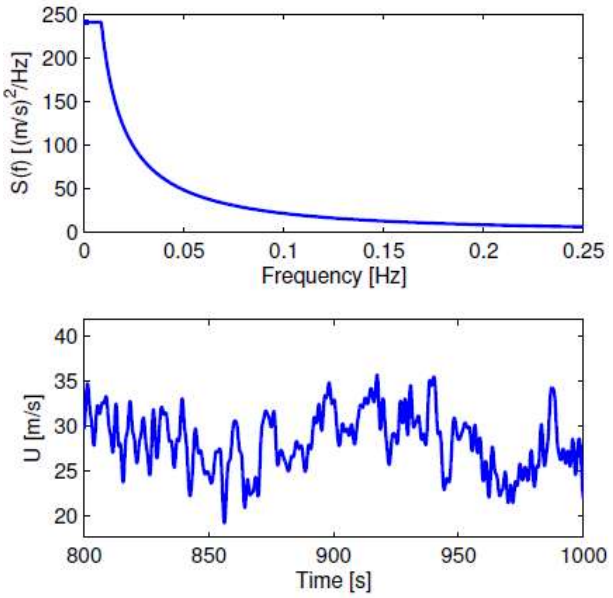

Figure 10. Chosen wind spectrum (above) and short realisation of wind speed (below)

Aerodynamic drag is calculated similarly to hydrodynamic drag,

$$dF_{aerodynamic} = \frac{1}{2}\rho C_d D U_{wind}{}^2 \qquad (10)$$

where $dF_{aerodynamic}$ is integrated along the structural element to obtain the aerodynamic load. C_d is the drag coefficient, D is the exposed diameter, U_{wind} is the wind velocity, modelled as a stochastic process,

$$U(t) = \bar{U} + \sum_{i=1}^{N} \sqrt{2S(\omega_i)d\omega_i}\, cos(\omega_i t + \varepsilon_i) \quad [12]$$

where $\bar{U}$ is the mean wind speed, ω_i denotes a discrete frequency, $S(\omega)$ is the frequency spectrum and $0 < \varepsilon_i < 2\,\pi$ is a uniformly distributed stochastic variable.

The Ochi & Shin offshore wind spectra [3] was chosen due to large energy content at low frequencies. The wind spectrum, along with a short realisation of the wind speed, is provided in Figure 10.

2.6 Environmental conditions

The 100 year return period environmental conditions considered in this study are shown in Table 2. All environmental loads are acting in the same direction transversal to the bridge.

Table 2. Environmental conditions

Wind-generated waves	Significant wave height [m]	3,3
	Peak period [s]	5,6
Swell	Significant wave height [m]	0,4
	Peak period [s]	16
Wind	Mean wind speed at 10m. height [m/s]	28,8
	Turbulence intensity [%]	12,5
Current	Surface speed [m/s]	0,7

3 Program Customization

New modelling capabilities have been developed in RM Bridge in order to account for hydrodynamic and hydrostatic loads. The hydro-static mass of the floater and the hydro-dynamic behavior of the structure had to be embedded in the existing time history analysis procedure for solving the non-linear equation of motion in time domain. RM Bridge uses the well-known Newmark algorithm for the solution.

3.1 Solution Procedure

All loads and interactions are considered inside the individual time steps using a Newton-Raphson iteration scheme for covering non-linearity. This implies full coupling of all loads throughout the time stepping procedure. The iteration process provides equilibrium in each time step with considering the force contributions from both inertia $M_a(\omega)$ and damping $C_A(\omega)$ as additional term $C(t)$ as shown in section 2.2.

This means that the convolution integral matrices $R(t)$ (*eq. 7 and 8*)) have to be solved in every iteration step. The integration task within the iteration steps was an enormous challenge for optimization of the calculation procedure to

achieve an acceptable performance. However, the reached performance and stability allowed for successfully performing the required investigations and studies tasks. Due the hydro-dynamic effects being concentrated at few degrees of freedom (floaters modelled as concentrated in one node) the increase of the calculation time is additionally limited.

3.2 Structural stiffness

A new element type "hydro-dynamic spring" has been introduced to manage the data transfer and calculation tasks. The properties of this special element describe the hydrodynamic stiffness as well as time dependent additional masses and damping behavior.

The hydro-static stiffness as shown in section 2.1 is given by density ρ, gravity constant g and the surface area A of the structure submerged in the water. It is to be entered as element property (generalized input of the 6 diagonal entries of the stiffness matrix).

3.3 Time Dependent Mass and Damping

Hydrodynamic mass and damping are defined as additional properties of these hydrodynamic spring elements. The hydrodynamic added mass and damping definitions in frequency domain are taken over from a 3rd party application ANSYS/AQWA. The data given in a right-hand coordinate system of AQWA has to be transformed to the RM Bridge left-hand system. This is done automatically in the import procedure without user interaction.

The constant part of the hydrodynamic mass $M_A(\infty)$ *(eq. 9)* is taken over from AQWA as a full symmetric mass matrix at the node representing the floater. This additional mass term is assembled to the global mass matrix. It influences the calculation of natural modes as well as the time history results.

The frequency dependent damping of the spring element is defined by the retardation function R(t) *(eq. 8)*. This frequency dependent damping is a non-symmetric and full matrix at the node.

In a first calculation step before the actual time history calculation is started, the frequency dependent damping is transferred into a time dependent damping. Solving the integral with respect to the given time step length in a pre-step allows saving calculation time during the Newmark integration. Assuming that the frequency dependent damping is given as a table of linearly distributed values c(ω), the integral can be evaluated analytically. There is no additional numerical inaccuracy introduced in this calculation step.

For the integration of the convolution integrals (*eq. 8*) which has to be executed during time history calculation, 3 alternatives have been implemented: using a trapezoidal rule (O(h)), a Simpson rule ($O(h^2)$) or cubic splines ($O(h^3)$). The best results in comparison with other programs were found with the trapezoidal approach.

The accuracy of the results is highly dependent on the input data and time step length. In our tests higher order integration did not give better results. Because of non-symmetry and because of embedding the new damping terms in an existing procedure, it has been decided to apply these terms as load on the right hand side of the equation system.

The integration has to be done within the non-linear calculation in every time step covering all non-linearity inside the iteration algorithm. The calculation is optimized by saving integrated terms that are constant for the current time step.

3.4 Wave Loading

Load terms in equation 6 are time, displacement, velocity or acceleration dependent, that means

$$F = F(t, u, \dot{u}, \ddot{u}) \tag{12}$$

First order wave forces (Froude Krilov and diffraction forces) and second order forces (mean drift forces, low frequency drift forces and summed high frequency forces) have been provided by a 3rd party application as frequency dependent tables. They may be entered as time dependent tables in the RM Bridge formula interpreter. This required a beforehand transformation from frequency domain into time domain by the user.

An alternative way of definition has been provided. A table of functions entered in the RM Bridge formula interpreter reduces the effort a lot.

Mathematical definition:

$$\varphi_1 = A_1 \cos(\omega_1 t) + B_1$$
$$\vdots$$
$$\varphi_n = A_n \cos(\omega_n t) + B_n$$
$$\varphi = \sum_{i=1}^{n} \varphi_i$$

Corresponding RM input (n, a_1, …, a_n, o_1,…, o_n, b_1, …, b_n set to actual values):

Table "phitab"		
	1	a_1*cos(omega1*t) + b_1
	….	….
	n	a_n*cos(omega$_n$*t) + b_n
Variable "phi"		tabsumB(phitab)

In order to efficiently considering these dependencies the internal formula interpreter of RM Bridge has been extended by the 3 functions: TDEFN(*node,dof,fact*), TVELN(*node,dof,fact*) and TACCN(*node,dof,fact*). These functions offer the possibility to adjust the factors of the applied loads during time history analysis. The program uses the current displacement, velocity or acceleration of the given node and degree of freedom at the time step begin, end or between, dependent on the given factor (0 – 1).

3.5 Current Loading

Fully coupled dynamic equation with viscous drag and time dependent loads are given in [2]. Viscous drag is relative to the structure motion and current velocity and can be described with the equation

$$q_{VDDE} = \frac{1}{2}\rho * C_d * D * (V_{stream} - V_{elem} * factor)^{\alpha} \quad (13)$$

A new load type (VDDE) has been implemented for considering this viscous drag forces. It takes the viscous drag profile on elements and cables into account, based on the current stream profile.

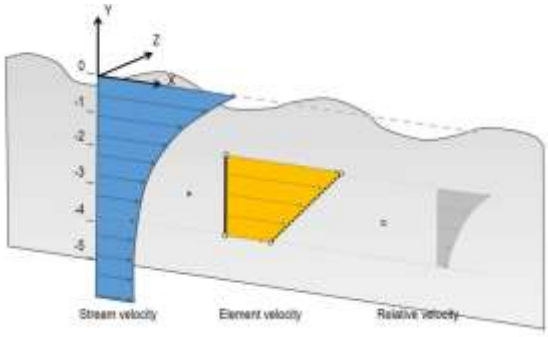

Figure 11. Distribution of wave loads and current forces over depth

The stream velocity can be entered flexibly as user defined table specified in the formula interpreter. The relative velocity is considered for fluid drag force calculation since the structure is moving.

4 Results

4.1 Eigenmode analysis

Eigenmodes including hydrodynamic added mass are found iteratively by updating $M_A(\omega)$ until ω matches the frequency of the respective mode. Convergence was found after 2-3 iterations for all modes. The first 5 eigenmodes, all in the transversal direction, are shown in Figure 12.

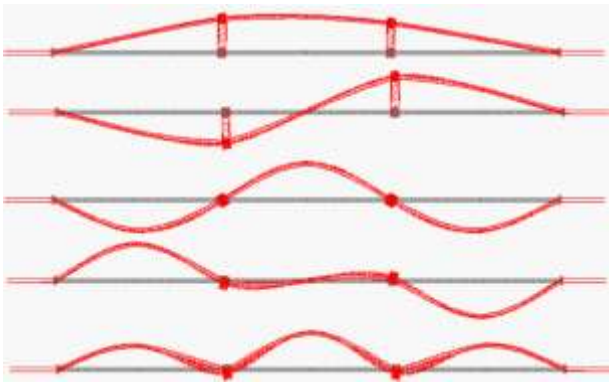

Figure 12. Eigenmode 1 to 5, viewed from above

The natural periods are provided in Table 3.

Table 3. Eigenperiods of the structure

Mode	1	2	3	4	5
Period [s]	81,6	56,4	17,6	15,4	13,1

The first two modes, which include significant motion of the floaters, are well below wave frequency excitation. This means that wave loads are mainly counteracted by inertial forces, limiting the wave induced motion of the floaters.

4.2 Wave response

Bridge response from coupled wave and current loading is shown in Figure 13. The current results in a static offset of less than half a metre. The motion amplitude of the floaters is small due to the large inertia. However, resonant excitation of mode 3 and 5 can be observed; the motion amplitude of the bridge deck mid span is several times larger than the amplitude of the floaters.

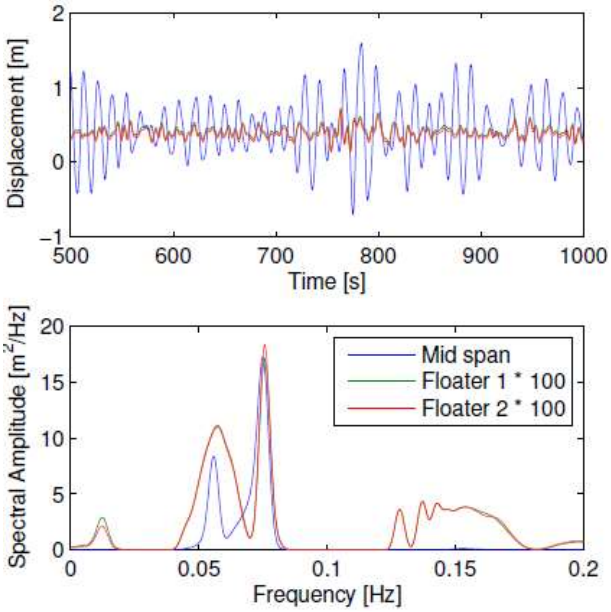

Figure 13. Transversal motion history (above) and frequency response spectra (below) of the bridge due to combined wave and current loading

4.3 Coupled wind and wave response

Bridge response from coupled wind, wave and current loading is shown in Figure 13. The dominant floater motion is in mode 1 and 2, while the bridge deck mid span shows response at modes 1, 3 and 5. This indicates that the global transversal bridge response is dominated by the wind loading.

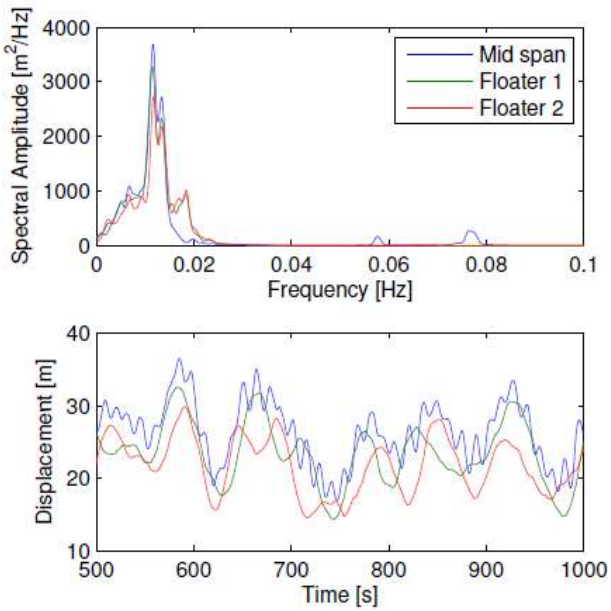

Figure 14. Transversal motion history (above) and frequency response spectra (below) of the bridge due to combined wind, wave and current loading

5 Conclusion and Future Work

The coupling of hydrodynamic effects with other non-linearity embedded in the Newmark scheme has been successfully implemented. This allowed for successfully performing the required feasibility studies related to hydrodynamic impact.

Wind effects have been simulated in a simplified manner. An extension of the project with respect to full coupling of aerodynamic effects in time domain has currently been started.

6 References

[1] Veie J., Holtberget S. Three span floating suspension bridge crossing the Bjørnafjord, proceedings at Multi-Span Large Bridges conference, Porto, 2015.

[2] Cummins W. E., The Impulse Response Function and Ship Motions, David Taylor Model Basin, Washington DC, 1962.

[3] DNV Recommended Practice C205, Environmental Conditions and Environmental Loads, DNV GL, Høvik, 2014.

[4] ANSYS AQWA Ver. 15.0, ANSYS Incorporated, Canonsburg, PA, 2012.